

# Vibrational Dynamics of Binary Metallic Glasses

A. M. Vora\*

Humanities and Social Science Department, STBS College of Diploma Engineering,

Opp. Spinning Mill, Varachha Road, Surat 395 006, Gujarat, INDIA

The theoretical investigation of the vibrational dynamics of two  $Zr_{67}Ni_{33}$  and  $Co_{67}Zr_{33}$  binary metallic glasses have been studied from model potential formalism using three different theoretical models proposed by Hubbard-Beeby (HB), Takeno-Goda (TG) and Bhatia-Singh (BS). Five local field correction functions viz. Hartree (H), Taylor (T), Ichimaru-Utsumi (IU), Farid *et al.* (F) and Sarkar *et al.* (S) are used for the first time in the present investigation to study the screening influence on the aforesaid properties. The pair potential is computed in Wills-Harrison (WH) form and used to study the Eigen frequencies of longitudinal and transverse phonon modes. The present results of phonon dispersion curves of  $Zr_{67}Ni_{33}$  glass is compared with the available MD results at different temperature. To explain electron-ion interaction pseudo-alloy-atom (PAA) model is applied for the first time instead of Vegard's Law. Further, thermodynamic and elastic properties have also been calculated from the elastic part of the phonon dispersion curves. Computed yielding of  $Zr_{67}Ni_{33}$  glass is found in fair agreement with the available data.

(Received February 23, accepted June 17, 2009)

*Keywords* : pair potential, glassy alloy, phonon dispersion curves (PDC), thermal properties, elastic properties.

## 1. Introduction

Recently due to the wide range of technological applications, there has been a great interest in the various properties of Zr and 3d or 4d transition metals based amorphous alloys. The interest in these materials stems partly from the fact that most of the Zr-rich amorphous alloys do not show a tendency to fracture, which makes them better starting materials for applications in high-field superconducting magnets than brittle crystalline alloys. Moreover, the thermal stability which gives consistent behaviour of these alloys is one of their most important properties. Also the research on intertransition metals based binary alloys has followed from the desire to understand the mechanisms responsible for their physical and electronic properties. Examples of

---

significant problems include the conditions under which amorphous or crystalline phases form, and the technological origins of negative temperature coefficients of electrical resistance. At a basic level all of these properties must be controlled by the electronic structure of the valence electrons. Theoretical understanding of these structures has been difficult to achieve because of the lack of translational symmetry, both for disordered crystalline alloys and amorphous or glassy alloys. The possible application of transition metal alloys is in microelectronics or as thin-film coating [1-7].

The theoretical calculations of phonon dispersion curves (PDC) of  $Zr_{67}Ni_{33}$  glass were studied by Gupta *et al.* [3] for the first time. They adopted Hubbard-Beeby (HB) [8] and Bhatia-Singh (BS) [9, 10] approaches in their study and compared the results with MD outcomes of Aihara *et al.* [1, 2]. They found their results are in good agreement with the reported data [1, 2]. Also, Otomo *et al.* [12] have studied the dynamical structure factor as well as collective excitations of this glass using NIS technique. Recently, Lad and Arun Pratap [4] have studied the PDC of five Zr-Ni alloys with model potential formalism using Takeno-Goda (TG) [11] and Bhatia-Singh (BS) [9, 10] approaches with Wills-Harrison (WH) form of pair potential [13]. Also, they have noted that, their results are found to be very close to those derived from MD and to the available experimental values [1, 2]. They have fitted the parameter of the potential with the experimental data in most of the cases. Very recently Vora *et al.* [14, 15] reported vibrational dynamics of some metallic glasses using model potential formalism. The PDC for  $Co_{67}Zr_{33}$  glass is reported first time in the present calculation. The experimental data of this glass is not available in the literature. In all these studies, the Vegard's law was used to explain electron-ion interaction for binaries. But it is well known that PAA is a more meaningful approach to explain such kind of interactions in binary alloys and metallic glasses [14-17]. Hence, in the present article the PAA model is used to investigate the phonon dynamics of  $A_{1-x}B_x$  (A : Co, Zr, B : Zr, Ni) binary glassy system.

Due to these facts, the theoretical computations of the vibrational dynamics of two metallic glasses viz.  $Zr_{67}Ni_{33}$  and  $Co_{67}Zr_{33}$  have been reported in the present article in terms of the two longitudinal and transverse modes at high as well as low values of wave vector transfer by employing three different well known approaches i.e. HB, TG and BS. The pair potential has been calculated using the Wills-Harrison (WH) [13] form of potential with well recognized model potential of Gajjar *et al.* [14-17]. Five local field correction functions viz. Hartree (H) [18], Taylor (T) [19], Ichimaru-Utsumi (IU) [20], Farid *et al.* (F) [21] and Sarkar *et al.* (S) [22] are used for the first time in the present investigation to study the screening influence on the aforesaid properties. The three approaches proposed by Hubbard-Beeby (HB) [8], Takeno-Goda (TG) [11] and Bhatia-Singh (BS) [9, 10] are used to generate the phonon dispersion curves (PDC). The thermodynamic and elastic properties such as longitudinal sound velocity  $v_L$ , transverse sound velocity  $v_T$ , isothermal bulk modulus  $B_T$ , modulus of rigidity  $G$ , Poisson's ratio  $\sigma$ , Young's modulus  $Y$ , Debye temperature  $\theta_D$  and low temperature specific heat capacity  $C_V$  have also been calculated from the elastic part of the PDC. Finally, a comparison is made between preset results and available experimental as well as theoretical data.

## 2. Computational Methodology

The fundamental component of the phonon dynamics of metallic glasses is the pair potential. In the present study, the pair potential is computed using Wills-Harrison (WH) approach [6, 15],

$$V(r) = V_s(r) + \left[ -Z_d \left( 1 - \frac{Z_d}{10} \right) \left( \frac{12}{N_c} \right)^{1/2} \left( \frac{28.06}{\pi} \right) \frac{2r_d^3}{r^5} \right] + Z_d \left( \frac{450}{\pi^2} \right) \frac{r_d^6}{r^8}. \quad (1)$$

The  $s$ -electron contribution to the pair potential  $V_s(r)$  is calculated from the relation given by [15],

$$V_s(r) = \left( \frac{Z_s^2 e^2}{r} \right) + \frac{\Omega_o}{\pi^2} \int F(q) \left[ \frac{\text{Sin}(qr)}{qr} \right] q^2 dq. \quad (2)$$

where  $\Omega_o$  is the atomic volume of the one component fluid.

The energy wave number characteristics appearing in the Equation (2) is written as [15]

$$F(q) = \frac{-\Omega_o q^2}{16\pi} |W_B(q)|^2 \frac{[\epsilon_H(q) - 1]}{\{1 + [\epsilon_H(q) - 1][1 - f(q)]\}}. \quad (3)$$

Here  $W_B(q)$ ,  $\epsilon_H(q)$ ,  $f(q)$  are the bare ion potential, the Hartree dielectric response function and the local field correction functions to introduce the exchange and correlation effects, respectively. In the present computation, the  $Z_s \sim 1.5$  is taken and another parameters  $Z_d$  and  $r_d$  are obtained from the band structure data [13].

The well characterized model potential  $W_B(q)$  of Gajjar *et al.* [14-17] used in the present computation is written as,

$$W_B(q) = \frac{-4\pi Z e^2}{\Omega_0 q^2 \varepsilon(q)} \left[ \begin{array}{l} \left\{ -1 + \frac{12}{U^2} + \frac{U^2}{1+U^2} + \frac{6U^2}{(1+U^2)^2} + \frac{18U^2}{(1+U^2)^3} - \frac{6U^4}{(1+U^2)^3} \right\} \cos(U) \\ + \frac{24U^2}{(1+U^2)^4} - \frac{24U^4}{(1+U^2)^4} \\ + \\ \left\{ \frac{6}{U} - \frac{12}{U^3} + \frac{U}{1+U^2} + \frac{3U}{(1+U^2)^2} - \frac{3U^3}{(1+U^2)^2} + \frac{6U}{(1+U^2)^3} \right\} \sin(U) \\ - \frac{18U^3}{(1+U^2)^3} + \frac{6U}{(1+U^2)^4} - \frac{36U^3}{(1+U^2)^4} + \frac{6U^5}{(1+U^2)^4} \\ + \\ 24U^2 \exp(1) \left\{ \frac{U^2 - 1}{(1+U^2)^4} \right\} \end{array} \right] \quad (4)$$

Where  $U = qr_C$  with  $r_C$  is the potential parameter. The detailed information of this potential is given in the literature [14-17].

The expressions for longitudinal phonon frequency  $\omega_L$  and transverse phonon frequency  $\omega_T$  as per Hubbard-Beeby (HB) [8] are,

$$\omega_L^2(q) = \omega_E^2 \left[ 1 - \frac{\sin(q\sigma)}{q\sigma} - \frac{6\cos(q\sigma)}{(q\sigma)^2} + \frac{6\sin(q\sigma)}{(q\sigma)^3} \right], \quad (5)$$

$$\omega_T^2(q) = \omega_E^2 \left[ 1 - \frac{3\cos(q\sigma)}{(q\sigma)^2} + \frac{3\sin(q\sigma)}{(q\sigma)^3} \right], \quad (6)$$

with

$$\omega_E^2 = \left( \frac{4\pi\rho}{3M} \right) \int_0^\infty g(r) V''(r) r^2 dr. \quad (7)$$

Following to Takeno-Goda (TG) [11], the wave vector ( $q$ ) dependent longitudinal and transverse phonon frequencies are written as

$$\omega_L^2(q) = \left( \frac{4\pi\rho}{M} \right) \int_0^\infty dr g(r) \left[ \left\{ rV'(r) \left( 1 - \frac{\sin(qr)}{qr} \right) \right\} + \left\{ r^2V''(r) - rV'(r) \right\} \right. \\ \left. \left( \frac{1}{3} - \frac{\sin(qr)}{qr} - \frac{2\cos(qr)}{(qr)^2} + \frac{2\sin(qr)}{(qr)^3} \right) \right], \quad (8)$$

and

$$\omega_T^2(q) = \left( \frac{4\pi\rho}{M} \right) \int_0^\infty dr g(r) \left[ \left\{ rV'(r) \left( 1 - \frac{\sin(qr)}{qr} \right) \right\} + \left\{ r^2V''(r) - rV'(r) \right\} \right. \\ \left. \left( \frac{1}{3} + \frac{2\cos(qr)}{(qr)^2} + \frac{2\sin(qr)}{(qr)^3} \right) \right]. \quad (9)$$

According to modified Bhatia-Singh (BS) [9, 10], the phonon frequencies of longitudinal and transverse branches are give by

$$\omega_L^2(q) = \frac{2N_C}{\rho q^2} (\beta I_0 + \delta I_2) + \frac{k_e k_{TF}^2 q^2 |G(qr_S)|^2}{q^2 + k_{TF}^2 \epsilon(q)}, \quad (10)$$

and

$$\omega_T^2(q) = \frac{2N_C}{\rho q^2} \left( \beta I_0 + \frac{1}{2} \delta (I_0 - I_2) \right), \quad (11)$$

with

$$\beta = \frac{\rho a^2}{2M} \left[ \frac{1}{r} \frac{dV(r)}{dr} \right]_{r=a}, \quad (12)$$

and

$$\delta = \frac{\rho a^3}{2M} \left[ \frac{d}{dr} \left( \frac{1}{r} \frac{dV(r)}{dr} \right) \right]_{r=a}. \quad (13)$$

The expressions of  $I_0$  and  $I_2$  are, with  $x = qa$ ,

$$I_0 = 1 - \frac{\sin(x)}{x}, \quad (14)$$

and

$$I_2 = \frac{1}{3} - \sin(x) \left[ \frac{1}{x} - \frac{2}{x^3} \right] - \frac{2 \cos(x)}{x^2}. \quad (15)$$

Other details of various constants used in Equations (10) and (11) are narrated in the literature [9, 10]. Here  $M$ ,  $\rho$  are the atomic mass and the number density of the glassy alloy while  $V'(r)$  and  $V''(r)$  be the first and second derivative of the pair potential.

The present study also includes the computation of longitudinal sound velocity  $v_L$ , transverse sound velocity  $v_T$ , isothermal bulk modulus  $B_T$ , modulus of rigidity  $G$ , Poisson's ratio  $\sigma$  and Young's modulus  $Y$ , Debye temperature  $\theta_D$  and low temperature specific heat  $C_V$  from the elastic limit of the PDC [15].

$$B_T = \rho_M \left( v_L^2 - \frac{4}{3} v_T^2 \right), \quad (16)$$

$$G = \rho_M v_T^2, \quad (17)$$

with  $\rho_M$  is the isotropic number density of the solid.

$$\sigma = \frac{1 - 2 \left( \frac{v_T^2}{v_L^2} \right)}{2 - 2 \left( \frac{v_T^2}{v_L^2} \right)}, \quad (18)$$

and

$$Y = 2G(\sigma + 1). \quad (19)$$

The Debye temperature is given in terms of both the velocities as [23],

$$\theta_D = \frac{\hbar \omega_D}{k_B} = \frac{\hbar}{k_B} 2\pi \left[ \frac{9\rho}{4\pi} \right]^{1/3} \left[ \frac{1}{v_L^3} + \frac{2}{v_T^3} \right]^{(-1/3)}, \quad (20)$$

here  $\hbar$  is the Plank's constant and  $\omega_D$  be the Debye frequency.

The low temperature specific heat  $C_V$  is obtained from Kovalenko and Krasny [24],

$$C_V = \frac{\Omega_0 \hbar^2}{k_B T^2} \sum_{\lambda=L,T} \int \frac{d^3 q}{(2\pi)^3} \frac{\omega_\lambda^2(q)}{\left[ \exp\left(\frac{\hbar \omega_\lambda(q)}{k_B T}\right) - 1 \right] \left[ 1 - \exp\left(-\frac{\hbar \omega_\lambda(q)}{k_B T}\right) \right]} . \quad (21)$$

The basic features of temperature dependence of  $C_V(T)$  are determined by the behavior of  $\omega_\lambda(q)$ .

### 3. Results and discussion

The input parameters and other related constants used in the present computations are narrated in Table 1. All the input parameters are calculated from the pure metallic data of the glassy alloy [10], while  $r_C$  is computed from the well known equation given by Heine and Weaire [25, 26]. The pair potentials, the phonon dispersion curves and the low temperature heat capacity of each metallic glass are displayed Figures 1-6.

The computed pair potentials of binary  $Zr_{67}Ni_{33}$  glass are shown in Figure 1. It is easily verifiable that the inclusion of exchange and correlation effect in the static Hartree dielectric screening changes depth and width of the pair potentials  $V(r)$ . The first zero for  $V(r = r_0)$  due to all screenings occurs at  $r_0 \approx 3.7$  atomic units (au). The  $V_{\min}(r)$  position is also affected by the nature of the screening. It is observed that well depth of presently computed potentials move towards the left as compared to the potentials of Gupta *et al.* [3].

The presently computed pair potentials of  $Co_{67}Zr_{33}$  glass are displayed in Figure 2. It is apparent from the figure that the inclusions of exchange and correlation functions affect significantly in the behaviour of the pair potentials. The first zero for  $V(r = r_0)$  due to all local field correction functions occurs at  $r_0 \approx 5.2$  au. The position of  $V_{\min}(r)$  is not highly affected by the nature of the screening and the oscillatory nature is also absent at large  $r$ -region.

From the Figures 1 and 2, it can be noted that the Coulomb repulsive potential part dominates the oscillations due to ion-electron-ion interactions, which show the waving shape of the potential after 10 au. Hence, the pair potentials converge towards a finite value instead of zero in repulsive region.

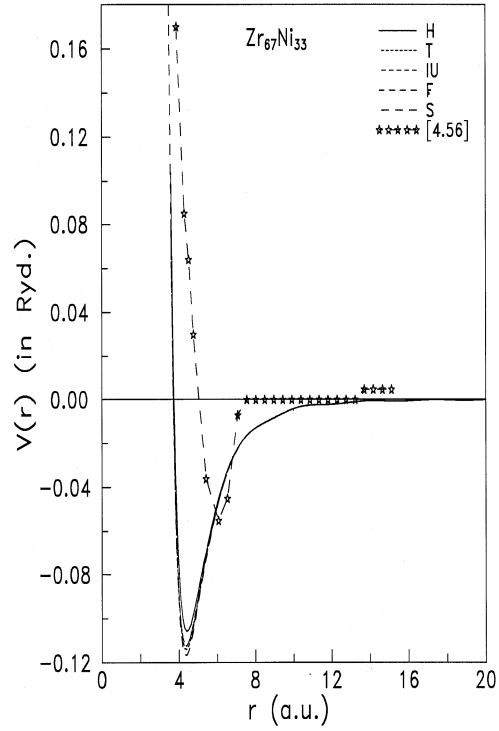


Fig. 1 Pair potentials for  $Zr_{67}Ni_{33}$  Glass.

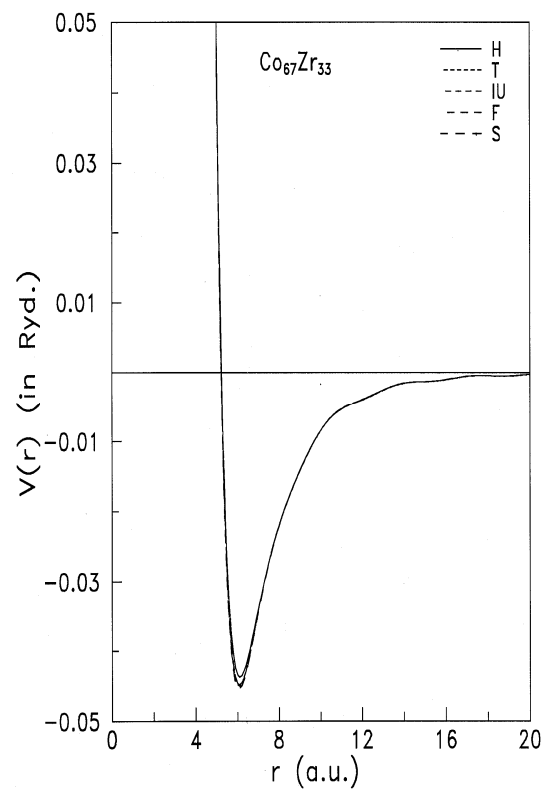
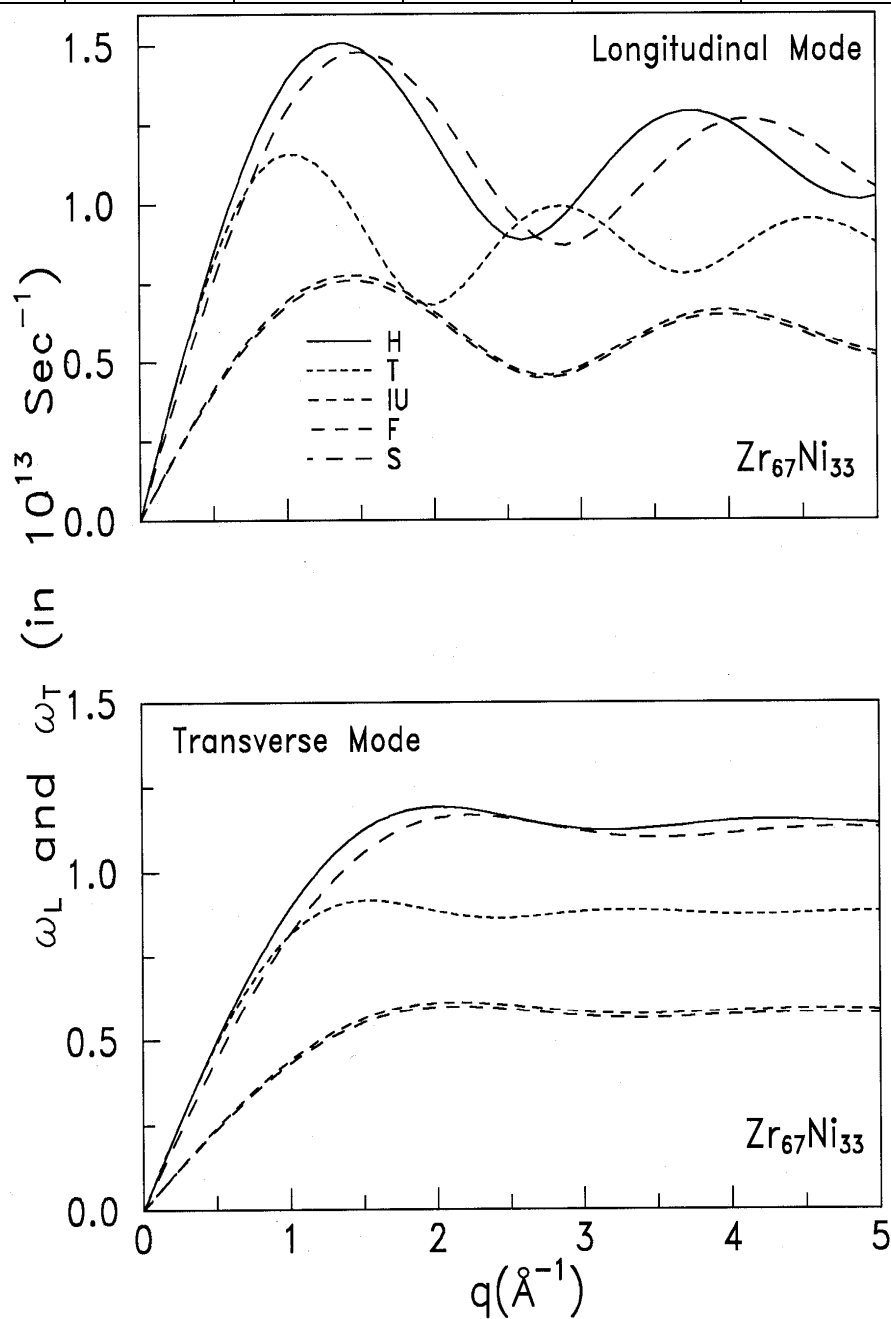


Fig. 2 Pair potentials for  $Co_{67}Zr_{33}$  Glass

Table 1 Input Parameters and constants.

Glass	Z	$\Omega_o$ (a.u.)	$r_c$ (a.u.)	$Z_d$	$N_c$	$r_d$ (a.u.)
Zr <sub>67</sub> Ni <sub>33</sub>	3.34	129.54	0.6889	4.48	12	2.23
Co <sub>67</sub> Zr <sub>33</sub>	3.33	102.59	0.7701	5.85	12	2.85

Fig.3 Screening influence on phonon dispersion curves of Zr<sub>67</sub>Ni<sub>33</sub> Glass.

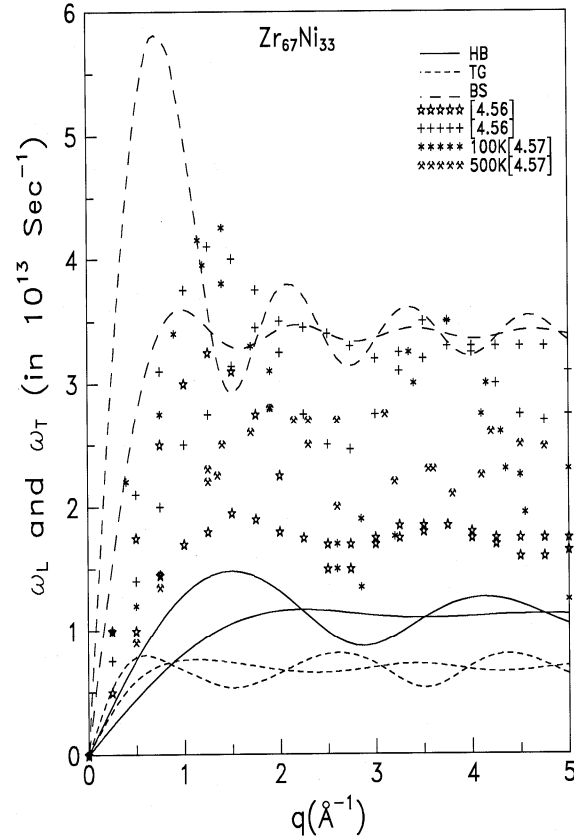


Fig. 4 Phonon Dispersion Curves for  $Zr_{67}Ni_{33}$  Glass.

The phonon dispersion curves (PDC) of binary  $Zr_{67}Ni_{33}$  glass computed using the HB approach with five screening functions and three approaches (HB, TG and BS) with S-local field correction function are shown in Figures 3 and 4, respectively. It is noticed from Figure 3 that, the inclusion of exchange and correlation effect suppresses the longitudinal as well as transverse phonon branches, in general. The first minimum in the longitudinal branch for H, T, IU, F and S-local field correction functions falls at  $q \approx 2.6 \text{ \AA}^{-1}$ ,  $2.0 \text{ \AA}^{-1}$ ,  $2.8 \text{ \AA}^{-1}$ ,  $2.8 \text{ \AA}^{-1}$  and  $2.9 \text{ \AA}^{-1}$ , respectively. The screening influence at first peak of  $\omega_L$  with respect to H-screening is 23.11% for T, 48.54% for IU, 49.62% for F and 1.86% for S-screening. Such influence on  $\omega_T$  due to T, IU, F and S-screening is 8.87%, 50.68%, 51.72% and 8.77% with respect to H – dielectric function at  $q \approx 1.0 \text{ \AA}^{-1}$  point, respectively. It is apparent from the Figure 4 that the oscillations are prominent in the longitudinal phonon modes only. The present yielding of PDC due to BS approach are higher than those of HB and TG approaches. The first minimum in the longitudinal branch occurs at  $q \approx 2.9 \text{ \AA}^{-1}$  for HB,  $q \approx 1.5 \text{ \AA}^{-1}$  for TG and  $q \approx 1.6 \text{ \AA}^{-1}$  for BS approach. The first crossover position of  $\omega_L$  and  $\omega_T$  in the HB, TG and BS approaches is observed at  $2.2 \text{ \AA}^{-1}$ ,  $0.8 \text{ \AA}^{-1}$  and  $1.3 \text{ \AA}^{-1}$ , respectively. The MD result of the Aihara *et al.* [1, 2] at two different temperatures 100K and 500K indicates the low and high amorphous states respectively, which are also shown in the same figure. It is interesting to note that the dispersion curves obtained through BS approach are found in qualitative agreement with the MD and theoretical results [1, 2]. Actually here model potential parameter  $r_c$  is

calculated from the well known formula, which shows significant difference than the reported data.

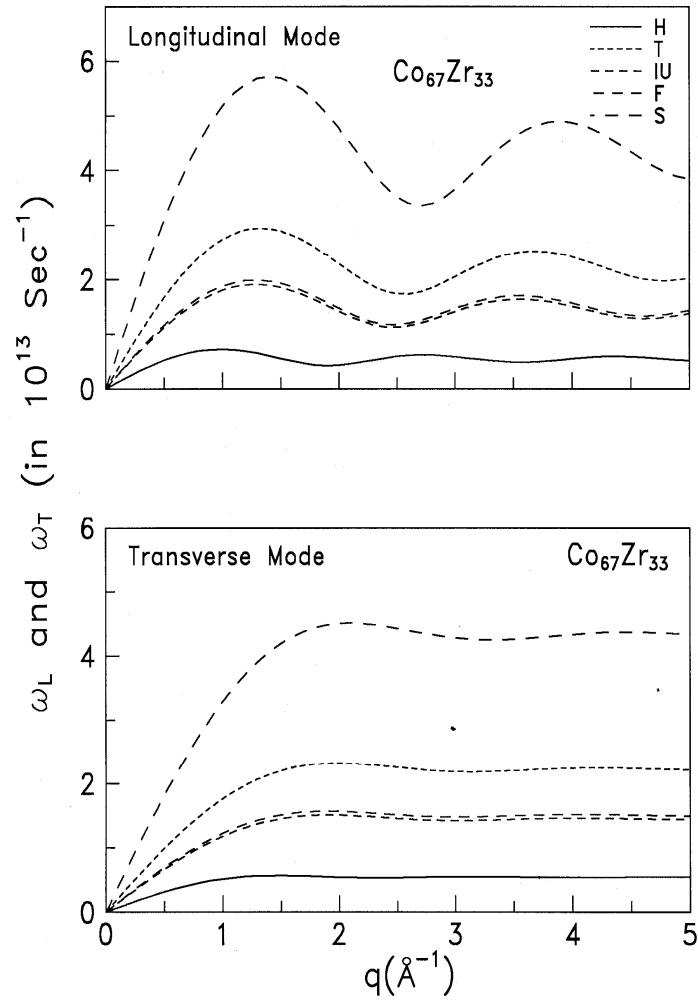


Fig. 5 Screening influence on phonon dispersion curves of  $\text{Co}_{67}\text{Zr}_{33}$  Glass.

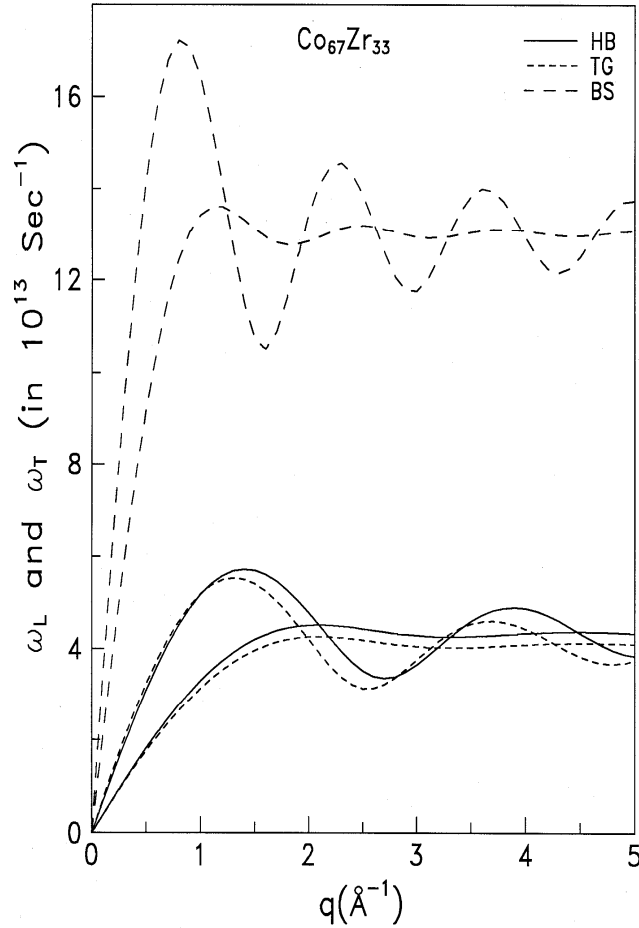


Fig. 6 Phonon Dispersion Curves for  $Co_{67}Zr_{33}$  Glass.

The results shown in Figure 5 is the phonon frequencies generated using HB approach with the five screening functions for studying the screening influence of  $Co_{67}Zr_{33}$  glass. It is seen that the inclusion of exchange and correlation effect raises the phonon frequencies in both longitudinal as well as transverse branches. The first minimum in the longitudinal branch is around at  $q \approx 1.9 \text{ \AA}^{-1}$  for H,  $q \approx 2.6 \text{ \AA}^{-1}$  for T,  $q \approx 2.5 \text{ \AA}^{-1}$  for IU as well as F and  $q \approx 2.7 \text{ \AA}^{-1}$  for S-local field correction function. The influence of local field correction functions on  $\omega_L$  at first peak due to T-dielectric function is 309.47%, for IU is 165.85%, for F is 176.63% and for S-screening is 695.93% with respect to H-dielectric function. Such screening variation on  $\omega_T$  at  $q \approx 1.0 \text{ \AA}^{-1}$  due to T, IU, F and S-screening is 242.98%, 128.17%, 137.40% and 539.75%, respectively. The PDC calculated from the HB, TG and BS approaches with S-local field correction function are shown in Figure 6 of  $Co_{67}Zr_{33}$  glass. The first minimum in the longitudinal branch falls at  $q \approx 2.7 \text{ \AA}^{-1}$  for HB,  $q \approx 2.7 \text{ \AA}^{-1}$  for TG and  $q \approx 1.6 \text{ \AA}^{-1}$  for BS approach. The first crossing position of  $\omega_L$  and  $\omega_T$  in the HB, TG and BS approaches is seen at  $2.1 \text{ \AA}^{-1}$ ,  $2.0 \text{ \AA}^{-1}$  and  $1.4 \text{ \AA}^{-1}$ , respectively. Moreover, the present outcome of PDC due to BS approach is higher than those due to HB and TG approaches.

It is noticed from Figure 7 that, the vibrational part of the specific heat ( $C_V$ ) is also influenced due to the inclusion of exchange and correlation effect for  $Zr_{67}Ni_{33}$  metallic glass. The high bump is observed in HB and TG approaches while such rise is absent in BS approach. Similarly, as shown in Figure 8, the modes of calculating phonon frequencies affect the anomalous behaviour of the specific heat ( $C_V$ ) for  $Co_{67}Zr_{33}$  glass. At low temperature region high bump is observed in HB and TG approaches, while linear nature is seen in BS approach. The 'anomalous linear' nature appears to be predominant in disordered materials containing low coordinated atoms. The computation of  $C_V$  is performed up to the elastic limits of the PDC i.e. low coordinated atoms only, which produced the 'anomalous linear' nature. After the elastic limit of the PDC atoms are highly oscillated, most probably which affected the nature of the  $C_V$ .

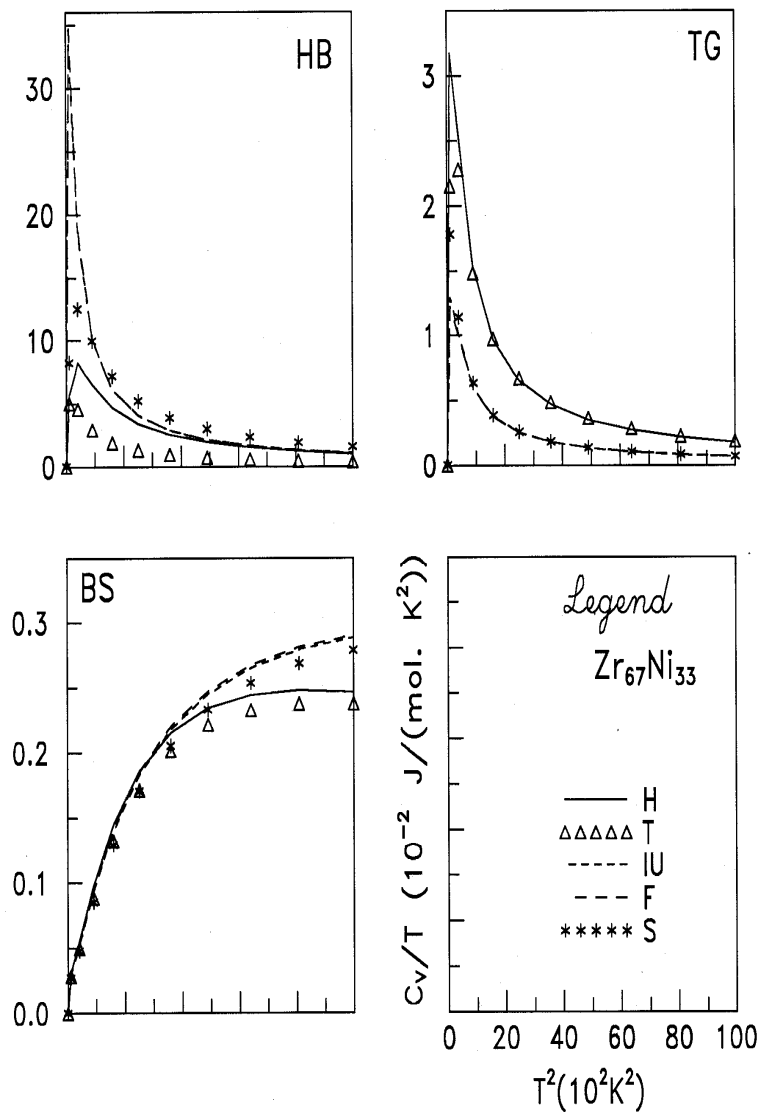


Fig. 7 The Vibrational Part of the Specific Heat ( $C_V$ ) of  $Zr_{67}Ni_{33}$  Glass.

The longitudinal as well as transverse sound velocities have been estimated from the linear part of the curves. The thermodynamic and elastic properties are calculated using both the sound velocities. All the computed results along with available theoretical data [1, 3] are listed in Table 2 for  $Zr_{67}Ni_{33}$  metallic glass. The velocities and  $\theta_D$  due to BS approach are closer to those of other data [1, 3], while another computed parameters show qualitative agreement with the reported one [1, 3].

Table 2. Thermodynamic and Elastic properties of  $Zr_{67}Ni_{33}$  metallic glass.

App.	SCR	$v_L \times 10^5$ cm/sec	$v_T \times 10^5$ cm/sec	$B_T \times 10^{11}$ dyne/cm <sup>2</sup>	$G \times 10^{11}$ dyne/cm <sup>2</sup>	$\sigma$	$Y \times 10^{11}$ dyne/cm <sup>2</sup>	$\theta_D$ (K)
HB	H	1.7890	1.0329	1.2466	0.7480	0.2499	1.8699	127.87
	T	1.8080	1.0438	1.2732	0.7639	0.2500	1.9099	129.23
	IU	0.8688	0.5016	0.2940	0.1764	0.2500	0.4410	62.10
	F	0.8507	0.4911	0.2819	0.1691	0.2500	0.4228	60.80
	S	1.5912	0.9187	0.9862	0.5917	0.2499	1.4793	113.73
TG	H	2.4117	1.3652	2.3357	1.3067	0.2642	3.3041	169.30
	T	2.8000	1.6136	3.0626	1.8256	0.2514	4.5689	199.80
	IU	2.7245	1.7035	2.4913	2.0347	0.1790	4.7979	209.26
	F	2.7767	1.7484	2.5479	2.1433	0.1715	5.0217	214.60
	S	2.4025	1.4765	2.0089	1.5284	0.1966	3.6576	181.70
BS	H	7.1769	3.4442	25.0234	8.3169	0.3504	22.4621	431.84
	T	7.2984	3.5679	25.4458	8.9254	0.3430	23.9732	446.91
	IU	7.2508	3.5201	25.2777	8.6874	0.3458	23.3835	441.08
	F	7.2261	3.5027	25.1404	8.6017	0.3464	23.1634	438.94
	S	7.3643	3.6236	25.7486	9.2059	0.3403	24.6768	453.72
Others [1, 3]		5.00	2.50	1.176	—	—	—	311
		4.19	2.05	0.846	—	—	—	256
		4.75	1.95		—	—	—	254 ± 11
								372.53

The longitudinal and transverse sound velocities have been calculated and reported for  $Co_{67}Zr_{33}$  glass in Table 3. It can be noted from the Table 3 that, all the properties calculated from the HB approach show minimum value, while those from the BS approach show higher values. Here, also the obtained yielding are more affected by the various screening function used in the present study as well as the approach adopted for generating PDC.

Table 3. Thermodynamic and Elastic properties of  $Co_{67}Zr_{33}$  metallic glass.

App.	SCR	$v_L \times 10^5$ cm/sec	$v_T \times 10^5$ cm/sec	$B_T \times 10^{11}$ dyne/cm <sup>2</sup>	$G \times 10^{11}$ dyne/cm <sup>2</sup>	$\sigma$	$Y \times 10^{11}$ dyne/cm <sup>2</sup>	$\theta_D$ (K)
<b>HB</b>	<b>H</b>	1.1669	0.6737	0.5780	0.3468	0.2500	0.8670	90.10
	<b>T</b>	3.5528	2.0512	5.3575	3.2145	0.2500	8.0363	274.31
	<b>IU</b>	2.3897	1.3797	2.4239	1.4543	0.2499	3.6358	184.50
	<b>F</b>	2.4865	1.4356	2.6242	1.5745	0.2499	3.9363	191.98
	<b>S</b>	6.5233	3.7662	18.0616	10.8370	0.2500	27.0924	503.65
<b>TG</b>	<b>H</b>	1.8757	1.0760	1.5086	0.8845	0.2548	2.2198	143.97
	<b>T</b>	4.0862	2.2450	7.6226	3.8505	0.2838	9.8867	301.44
	<b>IU</b>	3.0537	1.6901	4.2147	2.1824	0.2792	5.5834	226.81
	<b>F</b>	3.1567	1.7491	4.4964	2.3375	0.2785	5.9768	234.71
	<b>S</b>	6.8947	3.6996	22.3757	10.4569	0.2978	27.1425	497.63
<b>BS</b>	<b>H</b>	19.5280	11.9359	146.2232	108.8443	0.2018	261.6191	1587.56
	<b>T</b>	19.4162	11.8532	144.9000	107.3417	0.2030	258.2537	1576.75
	<b>IU</b>	19.4198	11.8601	144.8411	107.4662	0.2026	258.4731	1577.61
	<b>F</b>	19.4326	11.8688	145.0086	107.6246	0.2025	258.8377	1578.76
	<b>S</b>	19.3982	11.8373	144.7480	107.0543	0.2033	257.6454	1574.71

In all the three approximations, it is very difficult to judge that which approximation is the best for computations of vibrational dynamics of both metallic glasses, because each has his own identity. The HB approach is simplest and old one, which generating consistent results of the phonon data, because the HB approximation needs minimum number of parameters. While TG approach is developed upon the quasi-crystalline approximation in which effective force constant depends upon the correlation function for the displacement of atoms and correlation function of displacement itself depends on the phonon frequencies. The BS approach is retained the interatomic interactions effective between the first nearest neighbours only hence, the disorderness of the atoms in the formation of metallic glasses is more which show deviation in magnitude of the PDC as well as their related properties.

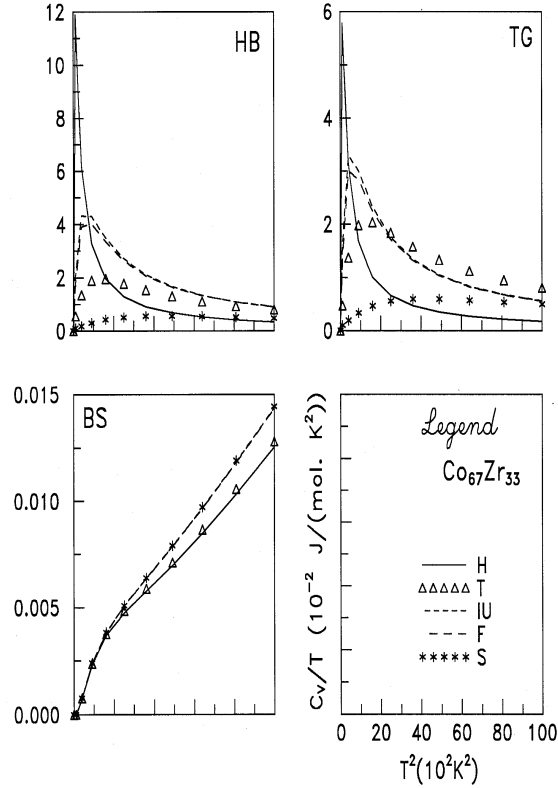


Fig. 8 The Vibrational Part of the Specific Heat ( $C_V$ ) of  $\text{Co}_{67}\text{Zr}_{33}$  Glass.

The dielectric function plays an important role in the evaluation of potential due to the screening of the electron gas. For this purpose in the present investigations the local field correction function due to H, T, IU, F and S are used. Reason for selecting these functions is that H – function does not include exchange and correlation effect and represents only static dielectric function, while T-function cover the overall features of the various local field correction functions proposed before 1972. The IU, F and S functions are recent one among the existing functions and not exploited rigorously in such study. This helps us to study the relative effects of exchange and correlation in the aforesaid properties. Hence, the five different local field correction functions show variations up to an order of magnitude in the Figures 1-8.

#### 4. Conclusions

Lastly it is conclude that, the study of phonon dynamics of both metallic glasses have not been investigated theoretically using the IU, F and S-local field correction functions previously. The comparison of present results of  $\text{Co}_{67}\text{Zr}_{33}$  glass is not made due to non-availability of theoretical or experimental data. But the present study is very useful to provide important set of the phonon data of  $\text{Co}_{67}\text{Zr}_{33}$  glass. These studies also confirm the applicability of the model potential in the aforesaid properties. Such study on phonon dynamics of other binary and ternary liquid alloys and metallic glasses is in progress, which will be communicated in near future.

---

**References**

- [1] T. Aihara Jr. and T. Masumoto, *J. Phys. Cond. Matt.* **7**, 1525 (1995).
- [2] T. Aihara Jr., Y. Kawazoe and T. Masumoto, *J. Non-Cryst. Sol.* **205-207**, 875 (1996).
- [3] Anuradha Gupta, Anamika Prasad, Deepika Bhandari, Kamal C. Jain and N. S. Saxena, *J. Phys. Chem. Sol.* **58**, 33 (1997).
- [4] Kirit N. Lad and Arun Pratap, *Physica B* **334**, 135 (2003).
- [5] Z. Altounian, Tu Guo-hau and J. Strom-Olsen, *J. Appl. Phys.* **54**, 3111 (1983).
- [6] M. P. Henaff, C. Colinet, A. Pasturel and K. H. Buschow, *J. Appl. Phys.* **56**, 307 (1984).
- [7] M. A. Engelhardt, S. S. Jaswal and D. J. Sellmyer, *Phys. Rev.* **B44**, 12671 (1991).
- [8] J. Hubbard and J. L. Beeby, *J. Phys. C: Solid State Phys.* **2**, 556 (1969).
- [9] A. B. Bhatia and R. N. Singh, *Phys. Rev* **B31**, 4751 (1985).
- [10] M. M. Shukla and J. R. Campanha, *Acta Phys. Pol.* **A94**, 655 (1998).
- [11] S. Takeno and M. Goda, *Prog. Thero. Phys.* **45**, 331 (1971); *Prog. Thero. Phys.* **47**, 790 (1972).
- [12] T. Otomo, M. Arai, J.-B. Suck and S. M. Bennington, *J. Non-Cryst. Sol.* **312-314**, 599 (2002).
- [13] J. M. Wills and W. A. Harrison, *Phys. Rev.* **B28**, 4363 (1983).
- [14] P. N. Gajjar, A. M. Vora and A. R. Jani, in *Proc. 9<sup>th</sup> Asia Pacific Physics Conf. Hanoi, The Gioi Publication, Vietnam, (2006)* 429.
- [15] Aditya M. Vora, *Chinese Phys. Lett.* **23**, 1872 (2006); *J. Non-Cryst. Sol.* **352**, 3217 (2006); *J. Mater. Sci.* **43**, 935 (2007), *Acta Phys. Pol.* **A111**, 859 (2007).
- [16] P. N. Gajjar, A. M. Vora and A. R. Jani, *Mod. Phys. Lett.* **B18**, 573 (2004); *Ind. J. Phys.* **78**, 775 (2004).
- [17] P. N. Gajjar, A. M. Vora, M. H. Patel and A. R. Jani, *Int. J. Mod. Phys.* **B17**, 6001 (2003).
- [18] W. A. Harrison, *Pseudopotentials in the Theory of Metals*, W. A. Benjamin, New York, 1966.
- [19] R. Taylor, *J. Phys. F: Met. Phys.* **8**, 1699 (1978).
- [20] S. Ichimaru and K. Utsumi, *Phys. Rev.* **B24**, 3220 (1981).
- [21] B. Farid, V. Heine, G. Engel and I. J. Robertson, *Phys. Rev.* **B48**, 11602 (1993).
- [22] A. Sarkar, D. Sen, H. Haldar and D. Roy, *Mod. Phys. Lett.* **B12**, 639 (1998).
- [23] J. Hafner, *Phys. Rev.* **B27**, 678 (1983).
- [24] N. P. Kovalenko and Yu. P. Krasny, *Physics* **B162**, 115 (1990).
- [25] V. Heine, D. Weaire, *Solid State Physics*, Vol. 24, Eds. H. Ehrenreich *et al.*, Academic Press, New York, 1970, p. 249.
- [26] J. Hafner, V. Heine, *J. Phys. F: Met. Phys.* **13**, 2479 (1983).